Advanced Steel Construction – Vol. 21 No. 6 (2025) 542–550
DOI:10.18057/IJASC.2025.21.6.7

EVALUATION OF MECHANICAL PROPERTIES OF NEW MODULAR STEEL CHANNEL TRUSS BEAMS UNDER ECCENTRIC LOADING

Shao-Chun Ma [1, 2, 3, *], Yi-Ming Liu [1, 3], Li Zhang [4] and Yun-Chi Xia [4]

[1] *School of Civil Engineering and Architecture / Kaifeng Research Center for Engineering Repair and Material Recycle, Henan University, Henan Kaifeng 475004, China*
[2] *Yellow River Laboratory (Henan), Henan Zhengzhou 450000, China*
[3] *Henan Province Research Center for Intelligence Conservation and Restoration of Historical Buildings, Henan Kaifeng 475004, China*
[4] *China Construction Seventh Engineering Bureau Co, Ltd, Henan Zhengzhou 450016, China*
** (Corresponding author: E-mail: scma@vip.henu.edu.cn)*

ABSTRACT

In order to address the challenges presented by the large size of conventional truss beams and the difficulties in hoisting, transportation, and installation. This paper proposes a new type of modular steel channel truss beams, which are formed by splicing the truss beam splices with high-strength bolts. This study conducted standard-load and overload destructive tests on six full-scale specimens under eccentric loads. It focused on the mechanical properties and damage characteristics of modular beams, along with evaluating the effectiveness of high-strength bolt splicing nodes. The results showed that the new type of modular steel channel truss beams possess excellent bending resistance and toughness. At the point where the ultimate bearing capacity is reached, the compression diagonal web buckles, causing damage to the modular beam. However, the high-strength bolt connection nodes remain intact. It shows that the overall toughness of the modular beam is significantly improved by the ability of the tensile action of connection nodes to absorb more deformation forces. The numerical model is established by simulation software and validated by comparing the calculations to the test results. The results are in close agreement, verifying the reliability of the finite element model. Additionally, the flexural performance of the modular beam is significantly influenced by the thickness of the compressed diagonal web. The flexural capacity of the composite beam depends on the critical load at which buckling damage occurs in the compressed diagonal web. Through numerical simulation, parameter optimization for the modular beam was conducted, and the optimal thickness of the compressed diagonal web was obtained. The calculation formula for the bending capacity applicable to the new modular beam is determined using the effective width method. This formula serves as the foundation for the theoretical design and practical engineering application of modular beams.

ARTICLE HISTORY

Received: 24 April 2024
Revised: 31 March 2025
Accepted: 6 May 2025

KEYWORDS

Channel steel modular beam;
Mechanical property;
Load-displacement curve;
High-strength bolt;
Numerical simulation

1. Introduction

Prefabricated construction is a product of the industrialization of the construction industry, which can achieve the goals of low energy consumption, short construction periods, high efficiency, and less pollution [1]. Compared to concrete structures, steel structures are lighter in weight, have lower foundation costs, and are more economical [2]. Steel is a ductile, versatile, and recyclable material [3]. Therefore, steel structures have significant development advantages and promising application prospects. It is of great significance for the healthy development of prefabricated buildings.

The integrated floor covering consists of compressed steel plate-concrete composite floor slab and channel steel truss beams. This design offers several advantages, including a reasonable force transmission path, high space utilization, and convenient pipeline arrangement [4-5]. As an important component of integrated building systems, truss beams have been extensively studied by scholars. Liu et al. [6] proposed a new type of double-layer steel-concrete combined wall with steel trusses as stiffening ribs. The steel truss enhances the steel plate's resistance to local buckling. Davis et al. [7] conducted an experimental study on an asymmetric I-beam floor structure using a full-scale model. The structure can withstand five times the live load under normal use. Hazal et al. [8] conducted full-scale tests and numerical simulations on steel-concrete composite trusses. They found that filling the compression chord members with concrete can effectively prevent local buckling. Leal et al. [9] proposed a steel-concrete composite floor slab system that consists of thin-walled steel trusses. The system can resist local buckling due to the collaboration of three different types of shear connectors, which provide sufficient stiffness and bending strength. Chen et al. [10] conducted a bending capacity test on five concrete floor slab specimens with lightweight steel truss beams. They found that the bending capacity of the floor slab was linearly related to the area of steel in tension and the height of the section. Jia et al. [11] evaluated the performance of truss beams and determined that the damage was primarily caused by the yielding of chord rods and the buckling of diagonal web rods. No significant damage was observed in the upper and lower columns and nodes. However, current research on truss beams primarily focuses on alterations in their mechanical properties when exposed to symmetrical loading. Modern engineering demonstrates that truss beams are influenced by various factors and complex forces. In their study of cold-formed steel roof frames, Doaa et al. [12] found that the loading method significantly impacts the bearing capacity, stiffness, and energy absorption capacity of the specimens. When two loading points are used instead of one, the energy dissipation capacity increases by 28%. Abdallah E et al. [13] found that the internal bending capacity of the face is significantly affected by the eccentric load in the numerical analysis of beam-CHS column-strut plate connection nodes. Cao et al. [14] simulation analysis of rectangular stainless steel tube concrete columns to investigate the impact of length-to-width ratio and relative eccentricity on the distribution of longitudinal stresses in the cross-section. The formula for calculating the compressive load capacity under eccentric load is provided. In conclusion, prolonged eccentric loading on truss beams can lead to a complicated stress scenario that could negatively impact the structure, posing a safety hazard [15-16]. Therefore, it is necessary to evaluate the performance of trusses under asymmetric loads to serve practical engineering.

Effective node connections are crucial for prefabricated concrete structures. Bolted connection nodes are widely used in practical engineering due to their convenience of construction and superior performance [17-18]. Elsabbagh et al. [19] conducted a parametric study of bolted semi-rigid nodes using the finite element method (FEM) and concluded that the shear values in the upper part of the connection significantly influence the mechanical properties of bolted connection nodes. Wang et al. [20] proposed a new type of bolted end plate connection (BEPC) for precast concrete column-column nodes. Low-cycle repeated loading tests demonstrated its excellent seismic performance, with minimal impact from the node position. Li et al. [21] proposed a formula for calculating the yield moment. They conducted low-cycle repeated loading tests on four foot-size specimens of bolted flange spliced nodes with varying flange thicknesses and different stiffening rib configurations. Fan et al. [22] conducted an experimental investigation into the performance and damage mechanism of a new type of self-tightening one-sided bolted node (STOSB). The seismic performance of this node is greatly affected by the end plate stiffness and column flange thickness. Liu et al. [23] conducted straight shear tests on bolted nodes to investigate the mechanical behavior and damage modes of bolted connections. The studies indicate that bolted connections can effectively reduce the deflection of truss beams and improve the overall comfort of the building's vibration [24]. It is recommended that bolted connections be used as much as possible in practical projects.

Currently, the truss beams used in real construction projects are typically monolithic. However, the substantial dimensions and weight of prefabricated components pose significant challenges to the standardization of production, transportation, and installation, as depicted in Fig. 1. The irrational design of truss beams, the occurrence of varying degrees of damage during transportation,

and the non-standardized installation of these components are prone to safety hazards to the engineering structure, and may even result in casualties or property losses, as illustrated in Fig.2. To address the aforementioned problems, this paper proposes a new type of modular steel channel truss beam spliced together with high-strength bolts. The force performance and damage mechanism were investigated through standard-load and overload destructive tests under eccentric loads. And analyzed the bending capacity through the finite element analysis tool for the extension study. The main factors that control the bending capacity were identified through theoretical analysis based on the principle of equal critical force.

Fig. 1 Hoisting of large-span steel truss

Fig. 2 Steel truss instability failure

2. Experimental design

2.1. Specimen design

The modular steel channel truss beam is a new type of beam commonly used in high-rise assembled monolithic floor cover structure systems, as shown in Fig. 3. It is the key component of the main structural floor plate force. To study its mechanical properties under standard-load and overload destructive tests, six full-scale specimens were designed and fabricated for two distinct groups, labeled E_i and F_i. Where: E represents standard-load test, F represents overload destructive test, and i = 1, 2, 3.

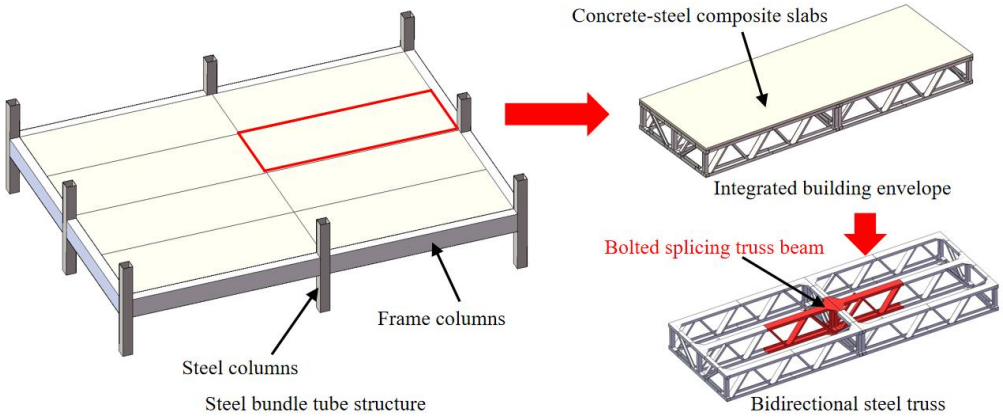

Fig. 3 Three-dimensional schematic diagram of new modular steel channel truss beam structure system

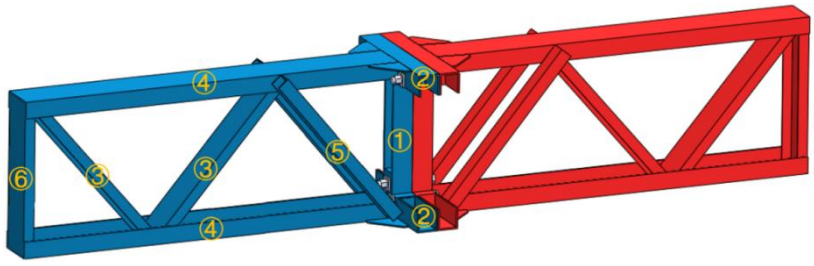

(a) Overall model

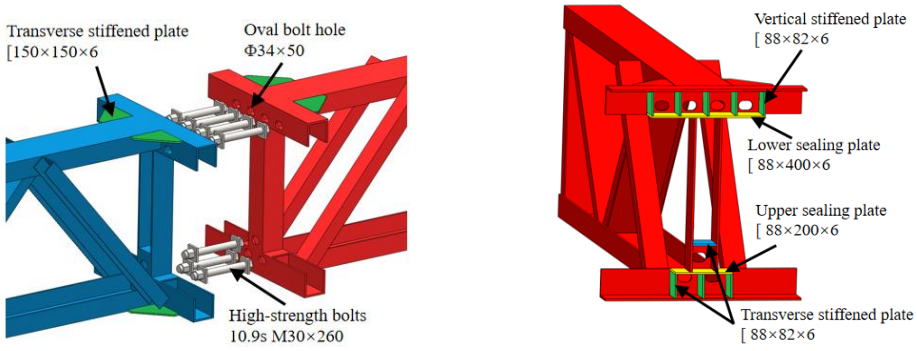

(b) Bolt splice node (c) Internal structure

Fig. 4 Three-dimensional schematic diagram of new modular steel channel truss beams

Referring to the design regulations of steel frame beams, supporting member regulations, and node structure requirements in GB50018-2002 Technical Code for Cold-Formed Thin-Walled Steel Structures [25] and Steel Structure Residential Main Component Dimension Guidelines 2020 [26], the

structure of the new modular steel channel truss beam is shown in Fig. 4, which consists of two identical main truss splices and seven sets of high-strength bolts. The members are constructed using Q345B channel steel. The top and lower chords of the main truss splice ① have a cross-section size of 200mm×80mm×8mm. The upper and lower chords of the secondary truss ②, which is perpendicular to the assembled main truss, have a cross-section size of 100mm×100mm×8mm. The end web ③ has a cross-section size of 150mm×50mm×4mm, while the vertical web ④ has a cross-section size of 100mm×100mm×8mm at the splicing location. The inner diagonal web ⑤ has a cross-section size of 180mm×50mm×4mm, while the outer diagonal web ⑥ has a cross-section size of 80mm×60mm×4mm. The bolt holes are reinforced with a 6mm thick lower sealing plate and a vertical reinforcement plate. Additionally, a 150mm×150mm×6mm horizontal reinforcement plate is installed at the intersection of the main truss and the secondary truss. High-strength, grade 10.9 friction-type bolts are utilized. Each group of high-strength bolts consists of a bolt rod, a nut, and two washers. The bolt rod has a diameter of 30 mm and a length of 260 mm.

In order to measure the displacement change of the specimen and the strain of the main rods during the loading process, it is essential to install the displacement meter, dial indicator, and strain gauges as shown in Fig 5.

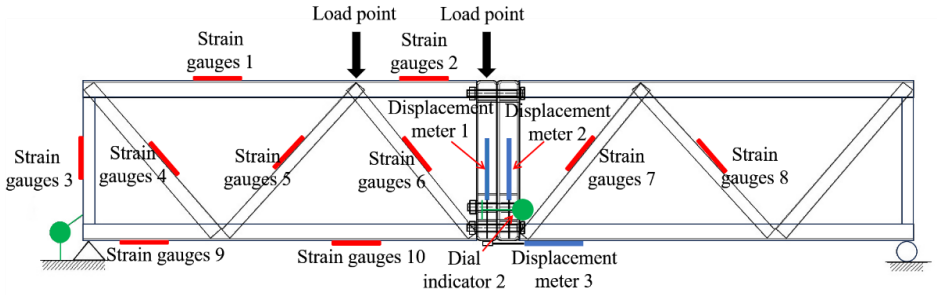

Fig. 5 Positions of measurement points

2.2. Loading set-up

The beam specimen underwent vertical loading using an electro-hydraulic servo-hydraulic loading system. To ensure a reasonable distribution and transfer of the load, the three-point centralized loading method was adopted. Eccentric loading was applied using loading blocks, with the eccentric loading points located at the splicing nodes of the modular steel channel truss beam and the intersection of the chords on one side. The hinged connection is formed between the two ends beam and the bearing. An anti-tipping device [27] is vertically arranged on the modular steel channel truss beam to restrict its out-of-plane deflection and prevent eccentric tipping during loading. The field-loading device is depicted in Fig. 6.

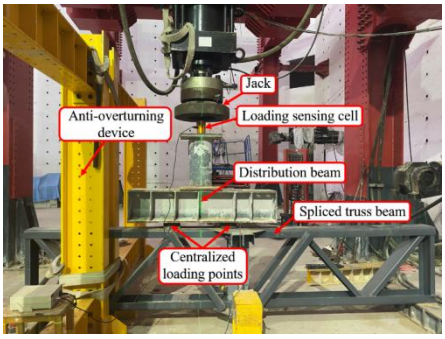

Fig. 6 Field loading device

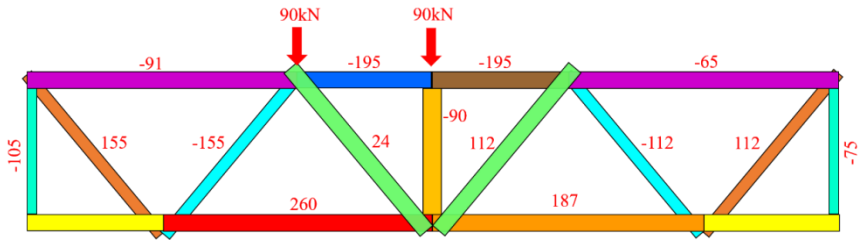

Fig. 7 Axial force diagram of the truss beam

2.2.1. Determine the bearing capacity for serviceability limit state

Before conducting the standard load test, it is necessary to determine the design value of the test loading by theoretically calculating the bearing capacity. To facilitate this calculation, the elastic deformation and constraint effect between adjacent bars are ignored. The node of the modular steel channel truss beam is regarded as a smoothly articulated node, and the axial force for each rod is calculated based on principles of structural mechanics. The calculation sketch is shown in Fig. 7. According to the specifications, the maximum tensile force of the lower suspension bar under standard combined load is 260 kN. In this load, the total value of the eccentric load corresponding to the upper part of the specimen is 180 kN, which is the maximum load limit for the standard load test.

2.2.2. Loading test

Pre-loading test: The pre-loading test is conducted on the specimen of the modular steel channel truss beam to eliminate any assembly gaps and verify the functionality of the testing equipment. The preloading load is controlled at 30% of the design load [28].

Standard load test: Each level of load increment is 10 kN, with a loading interval of 10 minutes. The load is incrementally increased to the standard load of 180 kN before being halted. 1 hour after unloading 20 kN at each level, the interval remains 10 minutes until completely unloaded.

Overload destructive test: The loading method and requirements are the same as the standard test. In the later stage, the load increment is 5 kN for each level, and the time interval remains unchanged. When the following conditions are met, the limit state of load-carrying capacity is considered to be reached, and loading is stopped: (1) specimen bars are bent or destabilized; (2) the maximum deflection reaches 1/50 of the support span [29].

3. Test results and analysis

3.1. Analysis of experimental phenomena

3.1.1. Standard load test phenomena

During the standard load test, the three specimens exhibited similar test phenomena. As the load increased during the early stage of loading, both the vertical displacement in the span and the tension displacement under the beam continued to increase. However, the vertical displacement in the span increased at a much faster rate than the tension displacement under the beam. When loaded to 180 kN, the vertical displacement in the span and the tension displacement under the beam reached their maximum values. The test results indicate that no relative slip occurred at each connection node, no tensile deformation occurred at bolted joints, and the specimen remained undamaged and in good condition. Under the action of eccentric load, the specimen can effectively and function normally within the design load range, meeting the specified requirements. During the unloading stage, the structural deformation gradually recovered as the load decreased. After complete unloading, the residual deformation was negligible. The results of the test are presented in Fig. 8.

(a) Pre-test (b) Load to 180kN (c) After unloading

Fig. 8 Standard load test

3.1.2. Overload destructive test phenomenon

Before loading to 180 kN, the test phenomena were not significant for each specimen. When the vertical load exceeded the design value, the beam still demonstrated stable flexural performance. As the load continued to increase, the displacement of the specimen gradually increased, indicating that it was in the elastic deformation state. At the load close to the ultimate bearing capacity of 327.9 kN, the beam experienced a sudden large deformation, accompanied by a loud ringing sound, destroying the member and the cessation of loading. The damage to the specimen is shown in Fig. 9. The test results indicate that yield deformation occurred first in the diagonal web on the eccentrically loaded side. The top channel steel of the vertical web bar bulged outward, and the upper chord bar buckled upward on both sides. Additionally, a downward bending phenomenon occurred in the middle of the span, resulting in obvious deflection deformation. The deformation characteristics of the rods were similar when the three specimens were damaged, as shown in Fig. 9(b)-(d). The main damaged parts are the compressed diagonal web bar on the eccentric loading side and the vertical web bar at the beam end. The stresses on both sides of the beam are uneven under the action of eccentric loading, indicating that different loading methods have a significant impact on the operational performance of the beams. Different loading methods of eccentric load have a great influence on the working performance of the beam. It is important to note that this analysis is based solely on objective evaluations and technical terminology. The deformation of the vertical web at the beam end occurred at the flange, while the web did not show obvious deformation. The primary reason is that the weak zone of the channel steel is located near the stress point in the opening, making it susceptible to bending and damage when compressed.

(a) Overall damage diagram for modular beams

(b) F1 localized damage diagram (c) F2 localized damage diagram (d) F3 localized damage diagram

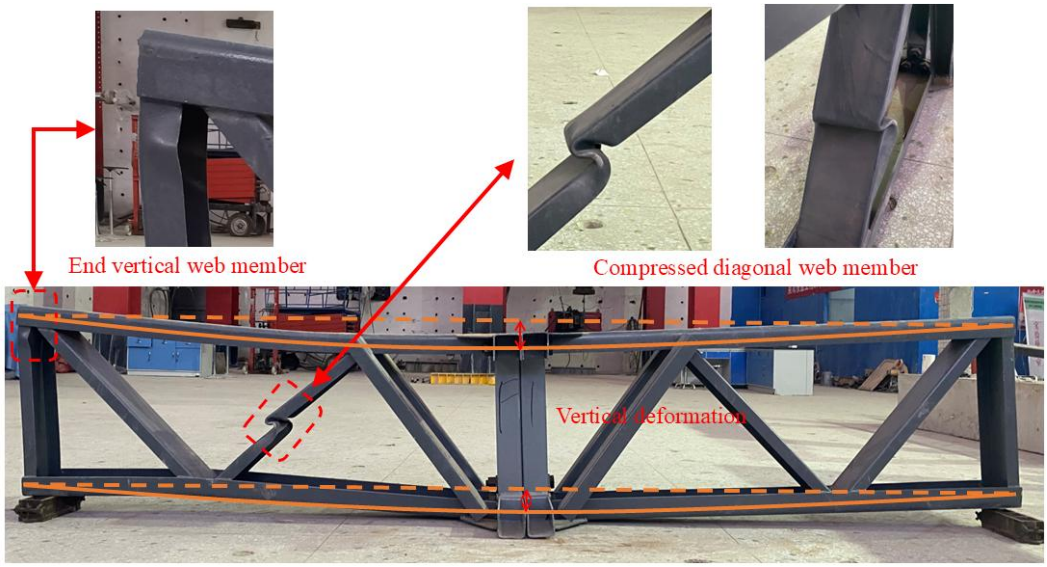

(e) Deformation and local failure of F1 specimen

Fig. 9 Damage diagram of modular steel channel truss beams

3.1.3. Failure analysis of high-strength bolts

After unloading the test, the specimen was removed to observe the residual damage of the high-strength bolts under eccentric loading. Fig. 10(a) shows the splicing surface of the modular steel channel truss beam, with the bolt holes remaining intact. The contact part of the spliced surface did not show any significant damage, indicating that the high-strength bolts effectively fastened the connection and prevented relative slip on the spliced surface. Fig. 10(b) shows the disassembled high-strength bolts. The bending deformation of the bolt rods is not significant, indicating good resistance to bending and safety margins. The high-strength bolt connection is reliable and effective in the event of modular steel channel truss beam destruction, making it suitable for practical engineering projects.

(a) Modular beam splice surface (b) High-strength bolts

Fig. 10 Damage diagram of splicing surface

Table 1
Main test parameters

	Standard load test								Overload destructive test					
No	P_y kN	δ_y mm	Δ_y mm	δ_r mm	Δ_r	δ_r/δ_y	Δ_r/Δ_y	No	P_u kN	δ_u mm	Δ_u mm	P_u/P_y	μ_y	Δ_u/δ_u
E_1	180.0	8.69	1.94	1.53	0.43	0.18	0.22	F_1	327.6	48.34	5.71	1.80	5.56	0.12
E_2	180.2	9.31	2.07	1.49	0.43	0.16	0.21	F_2	326.5	50.07	5.89	1.79	5.38	0.11
E_3	179.8	8.40	1.76	1.55	0.39	0.18	0.22	F_3	329.7	49.65	6.34	1.82	5.91	0.12
$\bar{E}$	180.0	8.80	1.92	1.52	0.42	0.17	0.21	$\bar{F}$	327.9	49.35	5.98	1.81	5.61	0.11

3.2. Load-bearing capacity analysis

The main test parameters obtained from the standard load test and the overload destructive test are shown in Table 1. P_y and P_u are the vertical loads for the serviceability limit state and the overload ultimate limit state, respectively. δ_y and δ_u are the mid-span deflections of the modular beams in these two limit states. Δ_y and Δ_u are the tensile sizes of the modular beam joints in these two limit states. δ_r and Δ_r are the mid-span deflections of the modular beams after complete unloading and the magnitude of tensors at the joints; μ_y is the modular beam ductility coefficient.

Table 1 shows that the vertical deflection of t the modular steel channel truss beam at the rod connection under the standard load is minimal, with an average value of 8.80 mm. According to Appendix A.1.1 of Code for Design of Steel Structures, the allowable deflection of bending truss members is $l/400$. The length of the combined beam is 3900 mm. The maximum allowable deflection can be calculated as 9.75 mm, and the vertical deflection of the combined beam meets the code requirements. The specimen joints do not show any apparent deformation, and the average tensile size is 1.92 mm. After complete unloading, the tensile sizes were reduced to 1.52mm, with a recovery rate of 83%. The beam's tension size is 0.42 mm, with a recovery rate of 79%. Within the normal load range, the deformation of the channel steel truss module beam specimen is relatively small, indicating good toughness.

In the overload destructive test, the modular steel channel truss beam exhibited a maximum vertical deformation of 49.35 mm and a ductility coefficient of 5.61. The ultimate load-carrying capacity was 327.9 kN, which is 1.82 times the ultimate load of normal use. This indicates that the modular steel channel truss beam has a sufficient safety margin. When the modular beam was damaged, the tensile size under the beam in the middle of the span was only 5.98 mm, which accounted for just 11% of the vertical displacement in the same location. This is because all the members of the modular beam adopt channel steel, with a relatively small moment of inertia of the cross-section and a relatively large slenderness ratio. Its tensile strength is much greater than its compressive strength. Under the action of loads, it is prone to compressive failure. The load acts directly on the upper chord bar. The upper chord bar is vertically compressed, while the lower chord bar is horizontally tensioned. Consequently, the vertical deformation of the upper chord bar is much larger than the horizontal elongation dimension of the lower chord bar. Meanwhile, the high-strength bolts effectively connected and fastened the beam, limiting its deformation in the middle of the span. It is recommended to promote the use of high-strength bolt connections in actual engineering applications of assembled buildings.

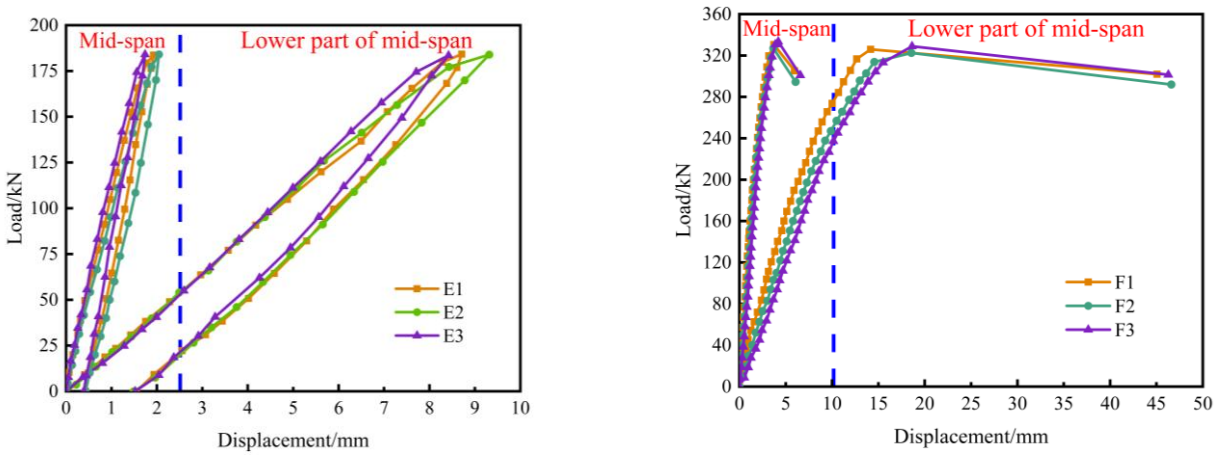

(a) Standard load effects (b) Over load effects

Fig. 11 Load-deflection curves in the mid-span

3.3. Load-displacement curve analysis

The load-displacement curves of the modular steel channel truss beam are shown in Fig. 11. It is not difficult to determine that the specimen is basically in the elastic working state during the standard load test, as the load-displacement relationship changes linearly. During the unloading process, the vertical displacement within the span and the tensile displacement beneath the beam of the specimen gradually decrease, while the slope of the load-deflection curve indicates a slow decrease. It indicates that the gap in the connection part of the specimen is not completely closed during the unloading process, which demonstrates its good energy absorption capacity and relatively ample safety margin.

From the analysis of Fig. 11, it can be seen that the specimen undergoes elastic and elastoplastic stages during the loading process of overload destructive tests. (1) Elastic Stage: At the beginning of loading, the relationship between load and displacement is linear. With the increase in load, the displacement gradually increases, and the standard load test is basically in the elastic-plastic stage. (2) Elastic-plastic stage: As the load is gradually increased to the ultimate load, the displacement growth rate accelerates. When the ultimate load is reached, the compression member of the modular steel channel truss beam undergoes buckling deformation. This results in a decrease in overall bearing capacity, as well as a significant increase in mid-span deflection and under-beam tensile displacement.

Under the same vertical load, the mid-span vertical displacement is much larger than the tensile displacement underneath the beam. Under the vertical load, the assembled main truss experiences the largest mid-span bending moment and deformation. During the overall stress analysis of the modular beam, the lower tensile displacement is relatively small, and the high-strength bolts exhibit good connection performance.

3.4. Load-strain curve analysis

Fig. 12 shows the load-strain curve of the modular beam. The measured strain is negative when the bar is compressed and positive when it is pulled during the test. Under eccentric load, the upper chord bar (where strain gauges 1 and 2 are located) is compressed, while the lower chord bar (where strain gauges 9 and 10 are located) is under tension. The diagonal web bar is under tension when inclined outward and under compression when inclined inward. The direction of the force of the vertical web bar is opposite to that of the diagonal web bar. The web bar inclined towards strain gauges 4, 6, and 7 is the tensile web bar, while the one inclined towards strain gauges 5 and 8 is the compressive web bar. The vertical web bar at the end of strain gauge 3 is under compression.

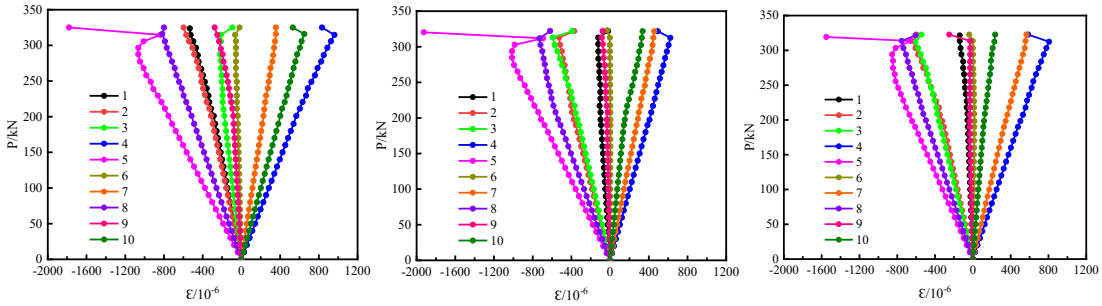

(a) Specimen F1 (b) Specimen F2 (c) Specimen F3

Fig. 12 Load-strain curves

By comparing and analyzing the load-strain curves in Fig. 13, it can be observed that the overall trend of the load-strain curves of the three specimens is essentially the same. During the entire loading process, the strains on the upper and lower chord bars are relatively small. The compressed diagonal web of strain gauge 5 is located at the eccentric loading point, where the strain growth rate is the largest. The strain growth rate of the tensile inclined web corresponding to strain gauge 4 is the second highest. During the overload destructive test, both the diagonal web bar of strain gauge 5 and the vertical web bar at the end of strain gauge 3 of the modular beam were damaged. Under the same load, the strain values of the compressed diagonal web bars were greater than those of the end vertical web bars. When the ultimate load was reached, both underwent abrupt changes. Therefore, under asymmetric loading, the compressed diagonal web buckled and was damaged before the end vertical web bar.

4. Parameter optimization and evaluation

In the overall stress process of the modular beam, the compressed diagonal web at the loading point is the first to reach the ultimate strength and damage. Therefore, the mechanical properties of the overall modular beam can be enhanced by strengthening the weak part. In order to investigate the main influencing factors of web size on the mechanical properties of the modular steel channel truss beam, the web thickness can be optimized. Except for the varying thickness of the compression-inclined web, all other parameters remain unchanged. The thickness (t) of the compression-inclined web is set at 4.5mm, 5mm, 5.5mm, 6mm, 6.5mm, and 7mm, respectively.

The load-displacement curves of modular beams with varying thicknesses of diagonal web bars are depicted in Fig. 13. As the thickness of the compression diagonal web increases, the stiffness and load-bearing capacity of the modular steel channel truss beam also increase, leading to a gradual reduction in mid-span deflection. When the thickness of the compression diagonal web is 5mm, the ultimate load-carrying capacity of the modular beam is 411.8 kN, which represents an increase of 16.59% compared to the initial value. When the thickness is 6mm and 7mm, the ultimate load capacity is 463.2kN and 472.2kN respectively, which is 31.14% and 33.69% higher than the initial value.

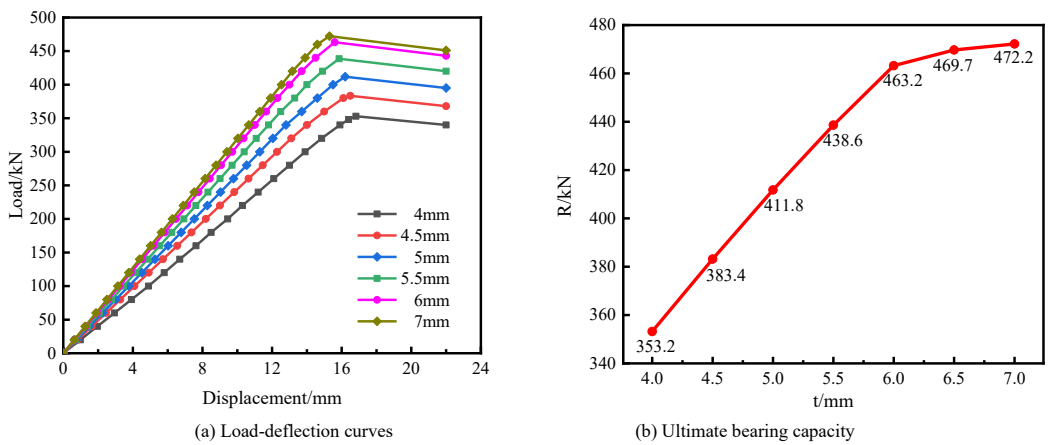

(a) Load-deflection curves (b) Ultimate bearing capacity

Fig. 13 Comparison of bearing capacity for different inclined web thicknesses

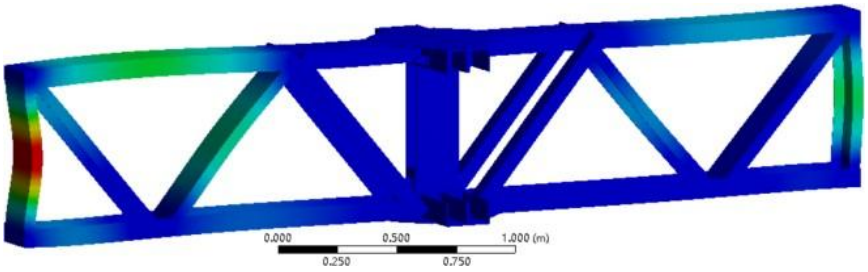

Fig. 14 Modular Beam Damage Patterns with compressive web thickness of 7mm

When the web thickness is less than 6mm, the ultimate load-carrying capacity of the modular beam is linearly related to the web thickness. With the gradual increase in the web thickness, the rise in the load-carrying capacity of the modular beam gradually diminishes. The ultimate load-carrying capacity of the compression-inclined web thickness increases from 6mm to 7mm by only 1.9%. When the thickness of the compressive web is 7 mm, the damage condition of the modular beam is shown in Fig. 14. At this time, the compressed vertical web at the end of the modular beam has priority over the compressed diagonal web and is subject to damage. However, the material properties of the compressed diagonal web are not fully utilized. When the thickness of the compressed inclined web exceeds 6 mm, the impact of increasing the web thickness on the load-carrying capacity of the modular beam is not significant. In order to fully utilize the material performance and achieve better economic outcomes, the thickness of the pressurized inclined web should be controlled in the structural design.

5. The bending capacity calculation of modular beams

5.1. Theoretical model

The stress distribution of modular beams is relatively complex in practical engineering. Therefore, it is common to assume that the stiffness and bearing capacity of each rod and connection in the modular beam are infinite. Without considering the effect of rod deformation on the bearing capacity of the modular steel channel truss beam, it is regarded as an ideal truss for simplified calculations. The simplified calculation model of the modular beam is shown in Fig. 15. By comparing and analyzing the test results and finite element simulation results of the modular beam, it can be observed that the compressed diagonal web bar is the weakest part of the modular beam. When the compressive web bar reaches the critical buckling load, the frame's modular beam is damaged as a whole. Therefore, the overall flexural load capacity of the modular beam can be calculated by inversely analyzing the ultimate load capacity of the stressed diagonal web bar. This calculation is of significant importance for the theoretical design of the modular beam.

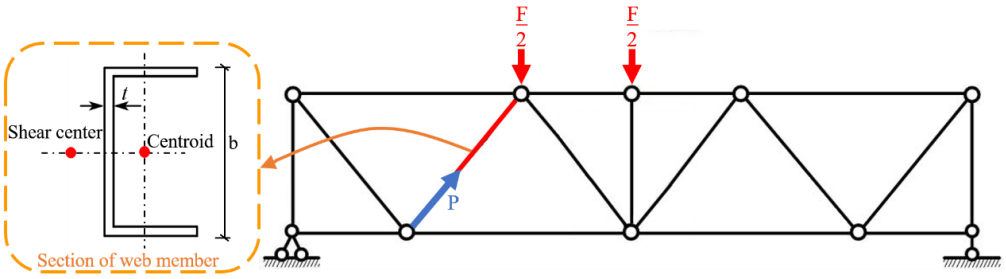

Fig. 15 Simplified computational model of modular beams

The modular steel channel truss beam with stressed diagonal web bars studied in this paper is a uniaxially symmetric channel. The shear center is located outside the back side of the channel, indicating that the axial pressure on the bar does not act on the shear center. When the bar is bent, torsional deformation occurs around the shear center, which is coupled with bending, resulting in bending and buckling of the bar. The critical load is less than both the bending critical load around the axis of symmetry and the pure torsional critical load.

The calculation of bending and torsional buckling is based on the principle of equal critical forces. This is achieved by converting it into bending and buckling of equivalent sections to determine the converted slenderness ratio. According to the Technical Specifications for Cold-Formed Thin-Walled Steel Structures, the stability coefficient is determined by meeting the requirements for bending buckling (axial compression bar). Additionally, the critical force for bending and twisting buckling is calculated. Formula (1) can be utilized to determine the critical buckling load of the compression diagonal web.

$$Pmax = \varphi A_e f \tag{1}$$

Conversion of length to slenderness ratio λ gets the length to slenderness ratio at its maximum value (maximum reduction degree), to wit:

$$\lambda = max\{\lambda_x,\ \lambda_y,\ \lambda_\omega\} \tag{2}$$

In the formula:λ_x ,λ_y is the length-to-finish ratio of the member to the x-axis and y-axis of the main axis of the cross-section;λ_ω is the converted length to slenderness ratio for bending and twisting flexure;

A_e is the effective cross-sectional area, The effective cross-sectional area is determined by first calculating the effective width of the compressed plate member using the effective width method.

$$b_e = \begin{cases} b_c & \dfrac{b}{t} \leqslant 18\alpha\rho \\ \left(\sqrt{\dfrac{21.8\alpha\rho}{b}} - 0.1\right) b_c & 18\alpha\rho < \dfrac{b}{t} < 38\alpha\rho \\ \dfrac{25\alpha\rho}{b} b_c & \dfrac{b}{t} \geqslant 38\alpha\rho \end{cases} \tag{3}$$

$$\alpha = 1.15 - 0.15\psi \tag{4}$$

$$\rho = \sqrt{205\frac{k_1 k}{\sigma_1}} \tag{5}$$

Where: b is the width of the plate; b_e is the effective width of the plate; ψ is the unevenness coefficient of compressive stress distribution; max compressive stress $\sigma_1 = \varphi f$; k is the coefficient of compressive stability of the plate; and k_1 is the plate group constraint coefficient.

In the simplified calculation model of the modular beam, the eccentric load F applied to the modular beam is calculated as 1.17 times of the axial force P of the compressed diagonal web bar using the structural mechanics solution. Therefore, the ultimate bending capacity $Fmax$ can be calculated according to formula (6).

$$Fmax = 1.17\varphi A_e f \tag{6}$$

5.2. Comparative analysis of theoretical and simulation results

Based on the results of the finite element analysis, it is evident that the compression-inclined web is the first part of the modular beam to sustain damage when its thickness is less than 6mm. Therefore, specimens with compression web thicknesses of 4mm, 4.5mm, 5mm, 5.5mm, and 6mm were selected for testing. The ultimate bending capacity ($Fmax$) was calculated and compared with the simulated ultimate bearing capacity (R) to draw valuable conclusions.

Table 2
Comparison of calculation and simulation results

No	t (mm)	$Fmax$ (kN)	R (kN)	$Fmax/R$	$(Fmax-R)/R$
1	4	363.9	353.2	1.03	3.03%
2	4.5	399.2	383.4	1.04	4.12%
3	5	430.5	411.8	1.05	4.54%
4	5.5	462.3	438.6	1.05	5.40%
5	6	495.3	463.2	1.07	6.93%
Mean				1.05	4.81%
Standard deviation				0.0146	0.0146

Table 2 shows that the calculated results of the compression-inclined web specimens with varying thicknesses closely align with the simulation results, with a ratio of 1.05, a standard deviation of 0.0146, and an average deviation amplitude of approximately 5%. It is concluded that the deviation rate tends to increase with the increase in web thickness. It is hypothesized that the error is due to the initial eccentricity of the modular beam under asymmetric loading. There appears to be a deviation between the calculated results based on the ideal articulated truss and the actual truss members. In addition, as the web thickness increases, the ultimate load capacity of the modular beam gradually rises, and the deformation of each member also increases. This aspect is neglected in the ideal modular beam model, leading to an increase in the deviation of the calculation results. Overall, the variance between the calculated and simulated results is relatively minor. It shows that the formula for the bending capacity of the modular beam, derived using the effective width method can be utilized in the design and calculation of new modular steel channel truss beams.

6. Conclusions

1. The new modular steel channel truss beam presented in this paper demonstrates improved bending resistance and toughness. The modular beam meets the normal use requirements stipulated in the code with high stiffness and low deformation. The results of the overload destructive test indicate that the ultimate bearing capacity exceeds the standard load by a factor of 1.82, while the ductility coefficient is 5.61, and the modular beam possesses a higher safety reserve capacity.

2. The shear performance of the high-strength bolt splicing node performs satisfactorily. While the new modular beam is damaged, the bending deformation of bolt rods and the slip of node splicing surface are not obvious. This indicates that using high-strength bolts for connections is relatively safe and enhances the modular beams' overall toughness. It is recommended to promote the application of high-strength bolt splicing nodes in practical projects.

3. According to the comparative analysis of the test and simulation results, the bending capacity of the modular beam depends on the critical load at which buckling damage occurs in the compressed diagonal web. On the premise of making full use of the material properties while taking economic factors into consideration, by increasing the thickness of the compressed diagonal web member from 4 mm to 6 mm, the ultimate bearing capacity of the new composite beam can be increased by 31.14%. This paper presents a formula for calculating the bending capacity of the new modular beam using the effective width method. The calculated results show a high level of concordance with the simulation results. The results can serve as a foundation for the structural, theoretical design, and practical engineering application of this new type of modular steel channel truss beam.

Acknowledgements

The authors would like to express heartfelt gratitude to the financial support by China Postdoctoral Science Foundation funded project (No. 2018M632805), Key scientific and technological project of Henan Province (No. 232102321066), Key scientific and technological project of Kaifeng City (No. 2303001).

References

[1] Li XJ, Xie WJ, Yang T, et al. Carbon emission evaluation of prefabricated concrete composite plates during the building materialization stage. Building and Environment, 2023, 232.110045. DOI:10.1016/j.buildenv.2023.110045.

[2] Khan K, Chen ZH, Liu JD, et al. State-of-the-Art on Technological Developments and Adaptability of Prefabricated Industrial Steel Buildings. Applied Sciences, 2023, 13(2): 685-685.

[3] Chen ZH, Khan K, Khan A, et al. Exploration of the multidirectional stability and response of prefabricated volumetric modular steel structures. Journal of Constructional Steel Research, 2021, 184.04022236. DOI:10.1061/JSENDH.STENG-11610.

[4] Simões SL, Silva LC, Tankova T, et al. Performance of modular hybrid cold-formed/tubular structural system. Structures, 2021, 30:1006-1019.

[5] Sangeetha P. Analytical Study on the Behaviour of Composite Space Truss Structures with Openings in a Concrete Slab. Civil and Environmental Engineering Reports, 2020, 30(3): 265-280.

[6] Liu ZH, Shu GP, Luo KR, et al. Performance of double-skin truss-reinforced composite wall under axial compression. Journal of Constructional Steel Research, 2023, 202.107778. DOI:10.1016/j.jcsr.2023.107778.

[7] Davis S, Stoddard E, Yarnold MT. Full-Scale Floor System Testing for Future Hot-Rolled Asymmetric Steel I-Beams. Journal of Structural Engineering, 2023, 149(2).04022236. DOI:10.1061/JSENDH.STENG-11610.

[8] Güldür H, Baran E, Topkaya C. Experimental and numerical analysis of cold-formed steel floor trusses with concrete filled compression chord. Engineering Structures, 2021, 234.111813. DOI:10.1016/j.engstruct.2020.111813.

[9] Leal L, Batista E. Experimental investigation of composite floor system with thin-walled steel trussed beams and partially prefabricated concrete slab. Const Steel Res, 2020, 172:106172. DOI:10.1016/j.jcsr.2020.106172.

[10] Chen Y, Quan CR, Feng L, et al. Experimental study on lightweight steel truss concrete slab. Building Science, 2020,36(01):54-60.

[11] Jia B, Ding J, Ding ZY, et al. Experimental Research on the Mechanical Behavior of Steel Frame Joints Using High-Strength Bolt Connection with Tapping Steel Plate. Progress in steel Building Structures, 2021,23(01):48-58.

[12] Bondok D, Salim H, Urgessa G. Quasi-static responses and associated failure mechanisms of cold-formed steel roof trusses. Engineering Structures, 2021, 231.111741. DOI:10.1016/j.engstruct.2020.111741.

[13] Abdallah E, El Aghoury Ihab, Mohamed IS, et al. Numerical investigation of branch plate-to-CHS connection under eccentric shear loading. Ain Shams Engineering Journal, 2023, 14(6).102139. DOI:10.1016/j.asej.2023.102139.

[14] Cao B, Zhu LF, Jiang XT, et al. An Investigation of Compression Bearing Capacity of Concrete-Filled Rectangular Stainless Steel Tubular Columns under Axial Load and Eccentric Axial Load. Sustainability, 2022, 14(14): 8946-8946.

[15] Wu CC, Fan FR, Cheng Z, et al. Behavior of steel reinforced UHPC-filled stainless steel tubular columns under eccentric loads. Journal of Constructional Steel Research, 2023,203.107806. DOI:10.1016/j.jcsr.2023.107806.

[16] Diao MZ, Guan H, Xue HZ, et al. Load-Resistant Mechanism and Failure Behaviour of RC Flat Plate Slab-Column Joints Under Concentric and Eccentric Loading. Springer Nature Singapore, 2023: 917-928.

[17] Yin LF, Niu Y, Quan G, et al. A numerical investigation of new types of bolted joints for cold-formed steel moment-resisting frame buildings. Journal of Building Engineering, 2023, 65.105738. DOI:10.1016/j.jobe.2022.105738.

[18] Guo XY, Amr R, Rahulreddy C, et al. Seismic Resistance of GFRP Bolted Joints with Carbon Nanotubes. Journal of Engineering Mechanics, 2018, 144(11): 04018106. DOI:10.1061/(ASCE)EM.1943-7889.0001528.

[19] Ashraf E, Tarek S, Salah N, et al. Behavior of extended end-plate bolted connections subjected to monotonic and cyclic loads. Engineering Structures, 2019, 190: 142-159.

[20] Wang ZQ, Xiong F, Chen J, et al. Experimental and Numerical Analyses on the Seismic Performance of a Novel Precast Concrete Column-column Joints with Bolted End-plate Connection. KSCE Journal of Civil Engineering, 2022, 26(11): 4746-4759.

[21] Tao YL, Chen XS, Liu XC. Seismic performance of CFST column bolted flange splice joints with connecting plates and rebar hooks. Engineering Structures, 2022, 267.114662. DOI：10.1016/j.engstruct.2022.114662.

[22] Fan SG, Xie SW, Wang K, et al. Seismic behaviour of novel self-tightening one-side bolted joints of prefabricated steel structures. Journal of Building Engineering, 2022, 56:104823. DOI：10.1016/j.jobe.2022.104823.

[23] Liu HL, Yang GY, Guo YJ, et al. Experimental Study on the Shear Deformation Characteristics and Mechanical Properties of Bolted Joints. International Journal of Geomechanics, 2023, 23(1). DOI:10.1061/(ASCE)GM.1943-5622.0002641.

[24] Zhang AL, Xie ZQ, Zhang YX, et al. Shaking table test of a prefabricated steel frame structure with all-bolted connections. Engineering Structures, 2021, 248. DOI:10.1016/j.engstruct.2021.113273.

[25] GB50018-2002 Technical code of cold-formed thin-wall steel structures. China Planning Press,

2002.
[26] Ministry of Construction of the People's Republic of China. Guide to the dimensions of main components for steel structure houses. China Construction Industry Press, 2021.
[27] Wang Y, Li T. Experimental and Numerical Investigation on Bending Capacity of Steel concrete Composite Truss Girder. The Open Civil Engineering Journal, 2015, 9(1): 943-949.
[28] Ma SC, Tan SL, Pan YH, et al. Experimental study on fiber-reinforced ceramsite concrete composite wall panel and correction of seismic damage model. Structures, 2024, 59: 105805.
[29] Liu WZ, Cui SQ. Experimental Study and Parametric Analysis on Flexural Performance of Bilateral Prestressed Composite Concrete Slabs with Steel Truss. Industrial Construction, 2021, 51(02):32-39+31.